**Department of Electronic & Telecommunication Engineering,**
**University of Moratuwa,**
**Sri Lanka.**


# Mini Project

## Pulse Oximeter

Submitted in partial fulfillment of the requirements for the module
BM4112 Medical Electronics and Instrumentation

Date: January 19, 2026

210218M Herath HMSI
210504L Rajapaksha NN
210720U Wijesinghe CD

# Contents

# 1 Introduction

Pulse oximetry is a non-invasive technique used to monitor arterial oxygen saturation ($SpO_2$) and heart rate by analyzing the optical absorption characteristics of blood. It is widely used in medical diagnostics due to its simplicity, safety, and real-time measurement capability. The method is based on the principle that oxygenated and deoxygenated hemoglobin exhibit different absorption spectra when illuminated with light of specific wavelengths [1].

This mini project focuses on the design and implementation of a pulse sensor system based on the photoplethysmography (PPG) signals. The system uses red and infrared light-emitting diodes (LEDs), a photodetector, analog signal conditioning circuitry, and a microcontroller to acquire and process PPG signals to obtain $SpO_2$ value. The objective of this project is to design a functional prototype capable of acquiring PPG signals, filtering noise, digitizing the data, and estimating $SpO_2$ levels. Main attention in this project is given on analog front-end design, signal integrity, and signal conditioning relevant to medical electronics.

# 2 Methodology

The system operation is based on photoplethysmography, which measures variations in blood volume by detecting changes in light absorption through biological tissue. Two wavelengths are used: red light (approximately 660 nm) and infrared light (approximately 940 nm). Oxygenated hemoglobin absorbs more infrared light, while deoxygenated hemoglobin absorbs more red light. In pulse oximetry two common approaches for optical path are present as transmission and refraction [2]. In this design, the transmission mode configuration was selected, with the LEDs and photodetector positioned on opposite sides of the tissue as it reduces the impact of direct optical leakage.

The red and infrared LEDs are alternately switched by the microcontroller, and the transmitted light through the finger is detected using a photodetector. The resulting current generated in the photodiode is proportional to the intensity of the received light and contains both DC and AC components. The DC component corresponds to absorption by tissue and venous blood, while the AC component corresponds to pulsatile arterial blood flow [3].

Following the photodetector, a low-pass filter is employed to cut off high-frequency noise. The output of this low-pass filter is utilized to extract the DC component, as the AC ripple is insignificant at this stage. Subsequently, a high-pass filter followed by an instrumentation amplifier is used to eliminate the DC component and obtain the amplified PPG signal. A sampling frequency of 100 Hz was selected to adequately capture the PPG waveform, which typically lies in the range of 0.5 Hz to 5 Hz. To calculate $R$, the values $AC_{Red}$ and $AC_{IR}$ are determined by taking the peak-to-peak value of the AC component (the output from the high-pass filter and amplifier), while $DC_{Red}$ and $DC_{IR}$ are calculated from the RMS value of the DC component (the output from the low-pass filter). Finally, the ratio-of-ratios method is used to derive $SpO_2$.

$$R = \frac{\left(\frac{AC_{Red}}{DC_{Red}}\right)}{\left(\frac{AC_{IR}}{DC_{IR}}\right)} \tag{1}$$

$$SpO_2 = A - B \cdot R \tag{2}$$

where $A$ and $B$ are empirically determined calibration constants.

The overall system architecture consists of an optical sensing unit, analog signal conditioning stage, microcontroller unit, and display interface. A block diagram of the system is shown in Figure 1.

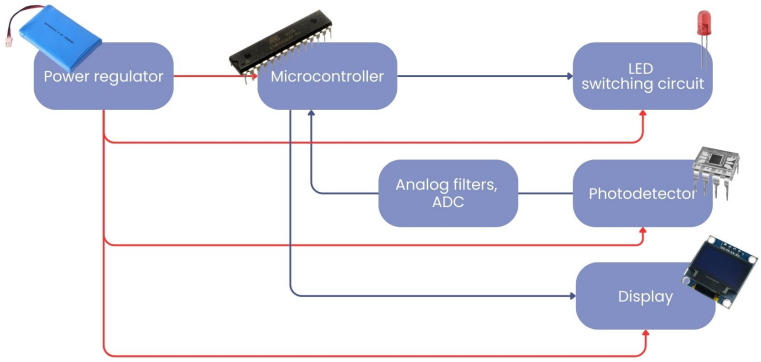


Figure 1: System block diagram of the pulse sensor

# 3 Design

## 3.1 Circuit design

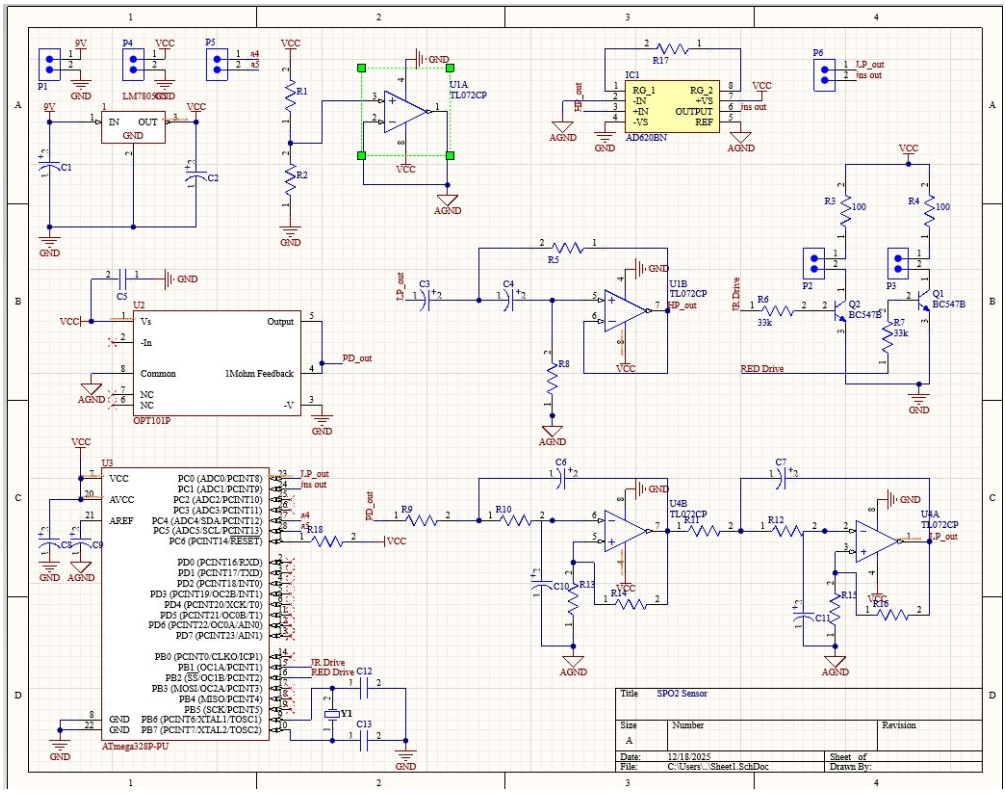


Figure 2: Schematic design

After finalizing the block diagram and overall interconnections, we proceeded to design the circuit and select the required components. The system was designed to operate on a 5V rail, while using a 2.5V mid supply reference as the analog ground. This mid supply bias is necessary because the AC components extracted

after the high-pass filtering stage must be centered within the ADC input range.

To power the circuit, we used a 9V battery and stepped it down using a 5V voltage regulator. A buffer circuit is then used to generate and isolate the 2.5V reference (analog ground), to prevent it from varying due to loading effects. We selected ATMEGA328P as the microcontroller.

LEDs are switched using microcontroller and photodiode output current is converted into a voltage using a transimpedance amplifier which comes with the built-in OPT101 [4] IC. Obtained signal is processed through cascaded active filters to isolate the DC and AC components of the PPG signal. A $4^{\text{th}}$ order Sallen-Key low-pass Butterworth filter with a cutoff frequency of 10.6 Hz is utilized to suppress high-frequency noise and extract the DC component. Subsequently, to eliminate the DC offset caused by ambient light and tissue absorption, a $2^{\text{nd}}$ order Sallen-Key high-pass Butterworth filter with a 0.47 Hz cutoff frequency is employed.

The AD620BNZ instrumentation amplifier [5] is then used to amplify the AC segment of the PPG signal. The TL072 [6] operational amplifier is used for the filter circuits. For tuning the gain 1 kΩ potentiometer is used in parallel with a 50 Ω resistor. So the maximum achieveble gain is, $G = \frac{49.4\text{k}\Omega}{R_G} + 1 = \frac{49.4\text{k}\Omega}{50} + 1 \approx 1000$.

The filtered and amplified signals from the low-pass output and the instrumentation amplifier are fed into the microcontroller's analog-to-digital converter (ADC) for further processing. The circuit schematic was designed using Altium.

## 3.2 PCB design

After the schematic was finalized with the component selected based upon availability, we proceeded to layout of the printed circuit board. A two layer configuration was used. The enclosure design was carried out simultaneously to make sure the PCB and enclosure fits together. This involved figuring out the mechanics of placing the finger. Upon finalizing the configuration, we decided to mount the photodetector on the PCB while keep the LEDs separate. These LEDs could then be mounted away from the photodetector so that the finger could be slid in between them. The final PCB layout is shown in Figure 6

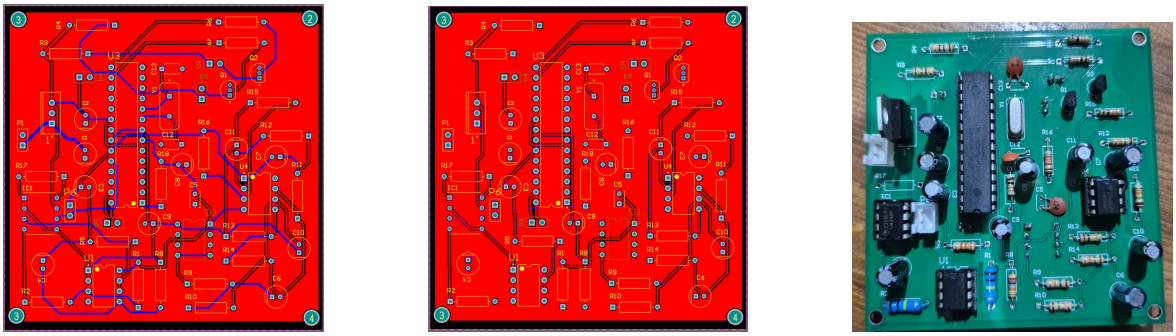

(a) PCB design top view (b) PCB design bottom view (c) Assembled PCB

Figure 3: Top and bottom views of the printed circuit board layout

## 3.3 Enclosure design

The enclosure was designed in series with the PCB layout to ensure mechanical compatibility and the proper functioning of the finger insertion mechanism. To accommodate the transmissive measurement method, a specific slot was created for finger placement. The LEDs are positioned on the upper side of this slot, while an aperture at the bottom allows transmitted light to reach the photodetector IC mounted on the PCB. The geometry is optimized to ensure the IC maintains direct contact with the bottom of the fingertip. Additionally, the enclosure incorporates the necessary features to mount the PCB, switches, battery pack, and OLED display. The final design is shown in Figure 4.

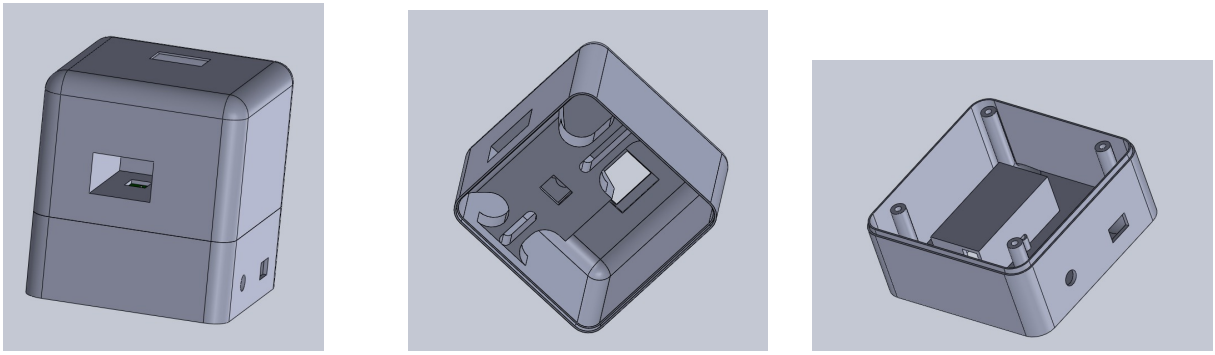

(a) Enclosure design (b) Enclosure top (c) Enclosure bottom

Figure 4: Enclosure design using Solidworks

The final design was then 3D printed and assembled by mounting the PCB, switches and the OLED display.

### 3.4 Firmware

The ATMEGA328P [7] microcontroller firmware was developed to manage LED switching, ADC sampling, and signal processing. The red and infrared LEDs are driven alternately via GPIO pins to ensure synchronized data acquisition, adhering to the switching sequence illustrated in Figure 5.

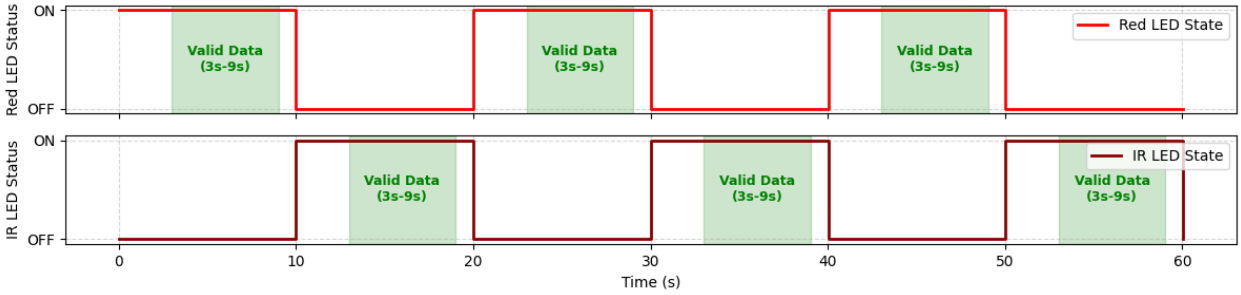


Figure 5: LED switching sequence and data acquisition window for SpO2 calculation

The microcontroller's ADC samples the conditioned signals at a frequency of 100 Hz. Samples are collected from both the low-pass filter output to extract the DC component and from the band-pass filtered instrumentation amplifier output to capture the AC component. To ensure signal integrity, data is exclusively processed within the 3 s–9 s window of each transmission cycle (indicated as "valid data" in Figure 5). This windowing strategy avoids the distortion in the PPG signal that occurs near the switching edges of the cycle.

The firmware calculates the signal components for both wavelengths: the AC component is derived from the peak-to-peak value of the amplified AC signal, while the DC component is determined using the RMS value of the low-pass filter output. These values are then used to compute the ratio required for $SpO_2$ estimation. The final $SpO_2$ reading is displayed on an external SSD1306 OLED module for real-time monitoring. The estimation formulas are provided below:

$$R = \frac{\left(\frac{AC_{Red}}{DC_{Red}}\right)}{\left(\frac{AC_{IR}}{DC_{IR}}\right)} \quad , \quad SpO_2 = 115 - 28.5 \cdot R \tag{3}$$

# 4 Testing and Measurement

Initial testing of the analog circuitry was conducted by simulatin on Multisim. After simulation, it is implemented on a breadboard to perform breadboard testing. Oscilloscope measurements were used to verify filter cutoff frequencies and signal amplitude. Then the complete schematic and PCB is designed using Altium circuit designer.

Figure 6a shows a typical PPG waveform obtained from the prototype. The waveform clearly demonstrates the pulsatile nature of arterial blood flow.

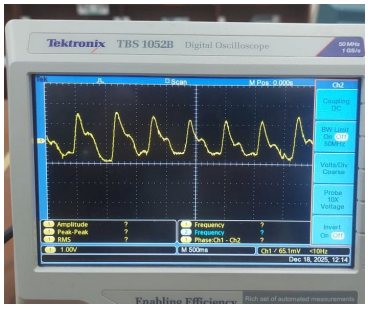


(a) PCG signal observed in Oscilloscope


(b) Integrated device bottom view

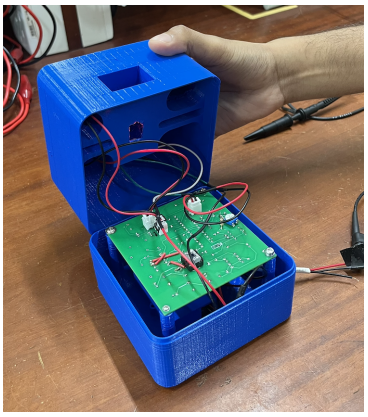

(c) Integrated device bottom view

Figure 6: Final integrated device and testing

After assembling the device we obtain data with the philips patient monitor and R ratio referred in Equation 1 values corresponding to our device from the same subject at the same time using index figures in left and right hands on different conditions. Since we could only select healthy subjects we could achieve ground truth labels in range 98 to 100. We used least squares fit to obtain parameter values described in Equation 2 as A=115 and B=28.5.

# 5 Conclusion

This mini project successfully demonstrated the complete design, implementation, and validation of a functional pulse oximetry system based on photoplethysmography. A full end-to-end pipeline was designed and implemented, including optical sensing, signal conditioning, analog to digital conversion along with integration with an enclosure. The use of dual-wavelength red and infrared LEDs in a transmissive configuration enabled reliable extraction of both AC and DC components of the PPG signal. Experimental results confirmed that the analog circuitry achieved adequate noise suppression, while synchronized LED switching and windowed data acquisition gave repeatable measurements. The observed PPG waveforms clearly exhibited physiological features, confirming the accuracy of the optical and electronic design choices.

Furthermore, the ratio-of-ratios method for $SpO_2$ estimation was implemented and calibrated using reference measurements from a clinical-grade patient monitor. The derived calibration constants produced $SpO_2$ values within the expected physiological range for healthy subjects, demonstrating good agreement with the reference device. Although the prototype was evaluated on a limited subject set, the results indicate that the system is capable of accurate oxygen saturation estimation under controlled conditions.

# References


[1] J. E. Sinex, "Pulse oximetry: principles and limitations," *The American journal of emergency medicine*, vol. 17, no. 1, pp. 59–66, 1999.

[2] M. W. Wukitsch, M. T. Petterson, D. R. Tobler, and J. A. Pologe, "Pulse oximetry: analysis of theory, technology, and practice," *Journal of clinical monitoring*, vol. 4, no. 4, pp. 290–301, 1988.

[3] A. Lu, T. Chen, L. Zhang, and E. Iqbal, "Pulse oximeter with digital readout of spo2 and heart rate," Course project report (BENG 186B: Principles of Bioinstrumentation Design), University of California San Diego, 2023, final project report (Group 4), hosted on the BENG 186B project archive. [Online]. Available: https://isn.ucsd.edu/courses/beng186b/project/2023/reports/group4.pdf

[4] *OPT101: Monolithic Photodiode and Single-Supply Transimpedance Amplifier*, Texas Instruments, Oct. 2003, originally published Jan. 1994; revised Oct. 2003. [Online]. Available: https://www.ti.com/lit/ds/symlink/opt101.pdf

[5] *AD620: Low Cost, Low Power Instrumentation Amplifier (Rev. E)*, Analog Devices, Inc., 1999, rev. E; 8-lead Plastic Mini-DIP (N), Cerdip (Q), and SOIC (R) packages. [Online]. Available: https://www.alldatasheet.com/datasheet-pdf/download/48090/AD/AD620.html

[6] *TL072: Low-Noise JFET-Input Operational Amplifier*, Texas Instruments, 2016, rev. J. [Online]. Available: https://www.ti.com/lit/ds/symlink/tl072.pdf

[7] *ATmega328P: 8-bit AVR Microcontroller with 32K Bytes In-System Programmable Flash*, Microchip Technology Inc., 2018, rev. 7810D–AVR–01/15. [Online]. Available: https://ww1.microchip.com/downloads/en/DeviceDoc/ATmega328P-Data-Sheet-7810.pdf